DESIGN OF A TOMATO PICKING ROBOTIC ARM BASED ON VISUALIZATION PLATFORM

Huiqin LI[1], Shuofei WANG[2], Shiguo XIE[3], Yangyang WANG[4], Pengfei WANG[5], Mingming LAN*[6]

In modern agricultural production, large-scale planting is commonly adopted. For the centralized and batch picking of fruits and vegetables during their mature period, specialized intelligent picking equipment is required. Various crops have different growth characteristics, and the picking environments are complex and diverse, necessitating different personalized picking equipment to meet different picking requirements. This paper designs and develops a visualization platform for the personalized design of picking robotic arms. It can optimize the relevant parameters of the robotic arm according to the workspace required for the picking of different crops, and efficiently complete the personalized design of the picking robotic arm in a short time. To verify the practicality of the visualization platform, in combination with the actual planting situation of tomatoes in greenhouses, the structural parameters of a tomato picking robotic arm are optimized and designed, and simulations and tests are carried out on its workspace and motion performance. The results show that the actual workspace and positioning accuracy of the tomato picking robotic arm meet the operation requirements. Moreover, during the actual operation process, it can move coherently and smoothly according to the preset trajectory, demonstrating good controllability and stability.

Keywords: visualization platform; picking robotic arm; personalized design; workspace; motion simulation

1. Introduction

The crop picking process is one of the procedures in agricultural production that is both labor-intensive and operationally complex. Modern agricultural production commonly adopts large-scale cultivation models. With the

[1] College of Mechanical and Electrical Engineering, Henan Agricultural University, Zhengzhou, China, e-mail: gaizanpvz922@163.com
[2] College of Mechanical and Electrical Engineering, Henan Agricultural University, Zhengzhou, China
[3] College of Mechanical and Electrical Engineering, Henan Agricultural University, Zhengzhou, China
[4] College of Mechanical and Electrical Engineering, Henan Agricultural University, Zhengzhou, China
[5] College of Mechanical and Electrical Engineering, Henan Agricultural University, Zhengzhou, 450002, China
[6] Corresponding author, College of Mechanical and Electrical Engineering, Henan Agricultural University, Zhengzhou, 450002, China, e-mail: lanming@henau.edu.cn

accelerated urbanization process in rural areas and the intensifying aging of the population, traditional manual picking methods have revealed numerous issues such as recruitment difficulties, high labor costs, heavy labor intensity, and low operational efficiency. Therefore, the use of intelligent picking manipulators to replace manual picking can effectively enhance crop picking efficiency and reduce labor costs, which is an inevitable trend in the development of modern agriculture [1-3].

In the 1960s, American scholars first proposed the idea of using robots to replace manual labor in harvesting operations and began to research related technologies for harvesting robots. After nearly two decades of technological development and practical experiments, by the end of the 20th century, countries such as China, Japan, and those in Europe also joined the research and development of harvesting robots one after another. This enabled harvesting robots to enter a stage of rapid development and achieve many research results [4,5]. Davidson et al. developed an eight-DOF apple harvesting robotic manipulator, comprising a six-DOF fully articulated arm integrated with a mobile base capable of planar x-y axis movement [6]. In addressing unstructured orchard environments, Silwal et al. proposed a seven-DOF harvesting manipulator featuring six sequentially arranged rotational joints complemented by a prismatic joint. The kinematic configuration was optimized through Monte Carlo simulations to determine optimal link lengths for target workspace requirements, with the base-mounted prismatic joint strategically incorporated for workspace expansion [7]. Lammers et al. innovated a dual-arm robotic harvester configuration, employing two coordinated four-DOF manipulators. This bimanual architecture demonstrates superior space efficiency and operational dexterity compared to conventional single-arm implementations [8]. Lehnert et al. developed a seven-DOF redundant robotic arm capable of autonomously harvesting sweet peppers in field cultivation environments. It consists of a 6-DOF rotational arm mounted on a prismatic lifting joint [9]. Williams et al. designed a novel multi-arm kiwifruit harvesting robot. The robot consists of four robotic arms specifically designed for kiwifruit picking, each equipped with a four-bar linkage mechanism as an end-effector, enabling safe kiwifruit harvesting in trellis-style kiwifruit orchards [10]. Hayashi et al. designed a three-DOF strawberry harvesting robotic arm for both soil cultivation and elevated substrate cultivation of strawberries. The robotic arm adopts an inverted structure with its lower part facing upward to provide space below the end-effector [11]. Wang et al. designed a P-P-R-P type continuous strawberry harvesting robotic arm to address the challenges of limited space and discontinuous harvesting in elevated strawberry cultivation. They conducted simulation tests using MATLAB software to analyze the robotic arm's workspace, along with the maximum velocity and acceleration variations of each joint [12]. Mehta and Burks developed a

seven-DOF citrus harvesting robotic arm, whose structure and shape mimic human arms to ensure flexibility and operational precision. A three-claw gripper is configured at the arm's end as the end-effector, capable of grasping citrus fruits of different sizes [13]. Henten et al. designed a four-DOF cucumber harvesting robotic arm for compact greenhouse cucumber cultivation environments. This robotic arm adopts a PPRR-type structure that effectively avoids collisions with plants and greenhouse structures [14]. Zhang et al. designed a six-DOF robotic arm for greenhouse cucumber harvesting, addressing the fragile nature of cucumber fruits and their random growth patterns. The arm is equipped with a visual servo system and two pneumatic flexible fingers, enabling autonomous cucumber harvesting operations [15]. Yang and Li developed a flexible grape harvesting robotic arm to tackle narrow and complex vineyard environments. The system combines a three-DOF SCARA robotic arm at the base with a flexible robotic arm at the top. Through kinematic analysis, simulation, and experimental verification, it was demonstrated that this robotic arm has a flexible structure and good motion performance, meeting the requirements for grape harvesting [16].

In conclusion, the robotic arms used in picking operations are usually self-developed. Through the personalized design of the robotic arms, they can adapt to the complex and diverse picking environments, thereby meeting different picking requirements [17]. In order to reduce the difficulty of the personalized design of the picking robotic arms and shorten the research and development cycle, this paper develops a visualization platform for the personalized design of the picking robotic arms. To verify the practicality of the visualization platform, in combination with the actual situation of tomato cultivation in greenhouses, a robotic arm suitable for tomato picking in greenhouses is designed and optimized, and a motion simulation analysis and a prototype test are carried out on it. The simulation and test results show that the actual workspace and positioning accuracy of the tomato picking robotic arm meet the operation requirements, and during the actual operation process, it can move smoothly according to the preset trajectory, demonstrating good motion performance.

2. Design and development of visualization platform

The visualization platform mainly meets the needs of personalized design of picking robotic arms. Users input the initial structural parameters of the picking robotic arm on the operation interface. Through human-computer interaction graphics, the simulation model and the workspace range of the corresponding picking robotic arm are intuitively displayed. In comparison with the picking operation requirements of crops, the initial structural parameters of the robotic arm are further evaluated and optimized. Finally, the structural parameters of the picking robotic arm that meet the picking requirements are determined. When using this platform for the personalized design of picking robotic arms, users do

not need to know the method of building the simulation model of the robotic arm and the algorithm for solving the workspace, which reduces the workload and development difficulty for designers and shortens the research and development cycle of the personalized design of the robotic arm.

The visualization platform needs to be constructed in three aspects: the function layer, the tool layer, and the data layer. The function layer realizes the personalized design of the robotic arm, as well as the visualization of the operation interface, simulation data, and simulation model. The tool layer mainly serves as a bridge connecting the function layer and the data layer. In this paper, App Designer in Matlab software is selected for the design and development of the visualization platform. It efficiently integrates the various functions defined by the function layer with the data provided by the data layer, constructing a complete visualization platform. The data layer focuses on constructing the internal program algorithms of the visualization platform. The D-H parameter method is utilized to build the coordinate system of the robotic arm. Subsequently, the kinematic simulation model of the robotic arm is developed via Matlab visual programming. The transformation matrix approach is employed to conduct a kinematic analysis of the robotic arm. Leveraging the Monte Carlo method, and based on the kinematic analysis results, the workspace of the robotic arm is simulated and calculated. As the pivotal algorithm within the visualization platform, the Monte Carlo method represents a numerical computation technique that relies on random sampling (pseudo-random values) to address mathematical and physical issues. Based on the theory of random probability, this method can avoid complex mathematical derivations and calculation processes, has a relatively fast calculation speed, and is easy to implement the graphic display function, making it suitable for solving the workspaces of various robotic arms. The basic idea of the Monte Carlo method for solving the workspace of the robotic arm is that when all joints traverse and take values within the corresponding value ranges, the set of all random values of the end point constitutes the workspace of the robotic arm.

The above algorithms have realized the data simulation analysis of the robotic arm, providing accurate and reliable data support for the personalized design and visual display of the function layer. The overall scheme design is shown in Fig. 1.

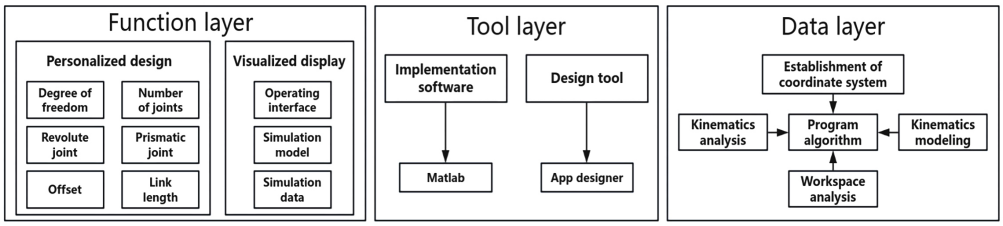

Fig. 1. Visualization platform scheme design

The implementation of the visualization platform involves multiple stages such as determining development tools, establishing program algorithms, designing the user interface, and writing callback functions, as shown in Fig. 2.

The user interface design of the visualization platform is divided into the design of the login interface and the main interface. Among them, the login interface includes an account password input area and an operation button area. Users can enter the main interface by inputting the account password and clicking the "Login" button. The main interface is divided into five areas. The coordinate graphic area is used to display the link coordinate systems and parameter descriptions of the manipulator. The parameter input area allows users to input relevant parameters of the manipulator according to the text prompts to obtain the parameter information of the manipulator. The progress display area is used to show the calculation progress of the manipulator's workspace. The operation button area enables users to build the simulation model of the manipulator and solve the workspace by clicking the operation buttons. Meanwhile, to prevent the overlap of original and new data, an initialization button has been implemented. The result display section showcases the finalized manipulator simulation model along with the determined workspace boundaries of the manipulator. In addition, when the "Exit" button is clicked, a message dialog box will pop up to determine whether to exit the platform, so as to avoid accidental exits caused by operational mistakes. The main interface of the visualization platform is shown in Fig. 3.

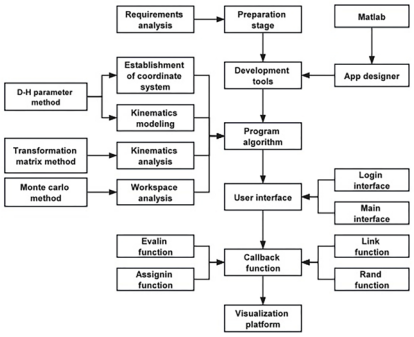

Fig. 2. Analysis of visualization platform

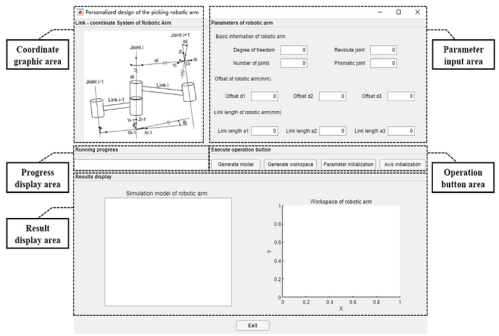

Fig. 3. Main interface of visualization platform

3. Design of tomato picking robotic arm based on visualization platform

Based on the independently designed and developed visualization platform for the personalized design of picking robotic arms, and combined with the actual situation of tomato cultivation in greenhouses, this paper designs a tomato picking robotic arm. Through the rapid configuration and optimization of the parameters of the robotic arm, the practicality of the visualization platform is verified.

Greenhouse tomatoes are crops cultivated in a vertical plane. Among its

numerous cultivation methods, ground cultivation is the most common. During the cultivation process, tomatoes grow vertically upward on the ground or in cultivation troughs, and with the help of trellises or stick-like support devices, the climbing and extension of the plants are achieved. Tomatoes in greenhouse sheds are planted in rows, with the row spacing of the plants being approximately 1.5 to 2 meters and the plant spacing being approximately 0.3 to 0.6 meters. The fruits are mainly distributed in the height range of 0.6 to 1.4 meters, as shown in Fig. 4.

According to the actual situation of tomato cultivation in greenhouses, combined with the parameters of the mobile platform carried by the picking robotic arm and the end-effector, a preliminary design of the tomato picking robotic arm is carried out. Its structural type is determined as a joint-type robotic arm with three degrees of freedom, and the working range is set to 500×500×800mm³. The specific initial parameters are as follows: the offset d1 = 50mm, d2 = d3 = 0mm, the link length a1 = 0mm, and a2 = a3 = 150mm.

Once the robotic arm parameters were initially set, the visualization platform was used to analyze and present the workspace of the tomato picking robotic arm. The X-axis range was roughly [-300, 300] mm, the Y-axis range about [-300, 300] mm, and the Z-axis range around [-100, 350] mm. When compared with the predefined working range for tomato picking tasks, it became evident that the workspace of this picking robotic arm was insufficient. It failed to encompass the area necessary for tomato picking operations, thus necessitating further parameter optimization.

Following several rounds of optimization, the details of the tomato picking robotic arm are illustrated in Fig. 5. The optimized X-axis workspace extended to approximately [-700, 700] mm, the Y-axis range reached about [-700, 700] mm, and the Z-axis range expanded to around [-200, 800] mm. These values met the design specifications.

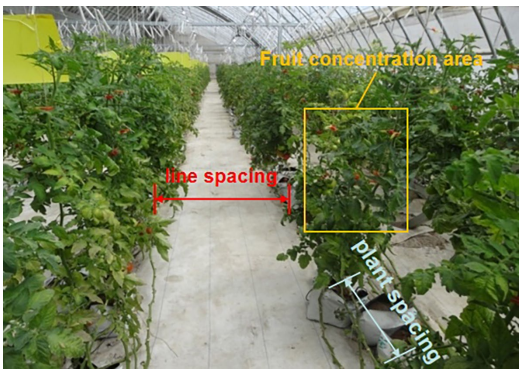

Fig. 4. Tomato planting situation in greenhouse

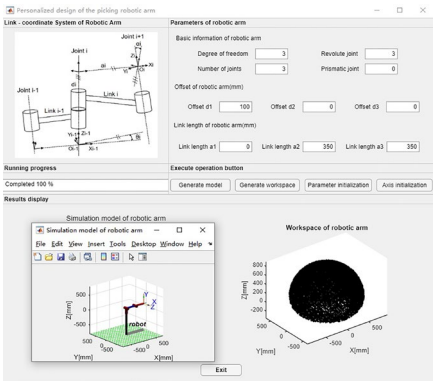

Fig. 5. Related information of the optimized tomato picking robotic arm

The workspace of the tomato picking robotic arm is approximately an

ellipsoid. Its size conforms to the parameter design of the arm itself, and the output distribution on each planar projection is uniform, without obvious cavities or voids. Meanwhile, it covers the range required for tomato picking operations in greenhouses, fully meeting the actual operation requirements. The three - dimensional diagram of its workspace and the planar projection diagrams are shown in Fig. 6. The red wireframe area in Fig. 6 represents the working range of the tomato picking robotic arm.

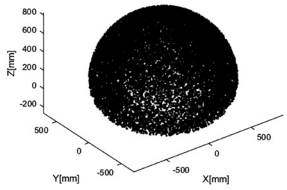

(a). Three-dimensional diagram of workspace

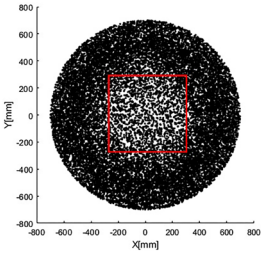

(b). Projection diagram of workspace on XY plane

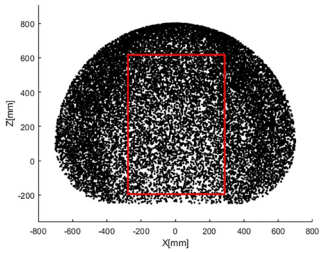

(c). Projection diagram of workspace on XZ plane

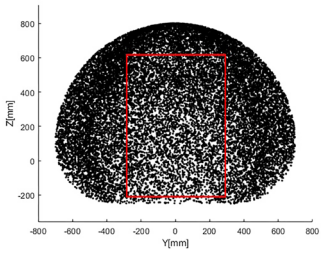

(d). Projection diagram of workspace on YZ plane

Fig. 6. Workspace of tomato picking manipulator

Using SolidWorks software, a 3D model of the tomato - picking robotic arm was created based on the parameters optimized and configured by the visualization platform, as depicted in Fig. 7. The tomato picking robotic arm designed in this study comprises three main components: the elbow joint, the shoulder joint, and the waist joint. The motors for the elbow and shoulder joints are positioned at either end of the shoulder joint. The elbow joint motor is linked to the driving arm via a harmonic reducer. Subsequently, the driving arm connects to the driven arm and the elbow joint, creating a parallelogram structure. The waist joint is attached to the base support, which, in turn, is connected to the motor through a worm gear reducer.

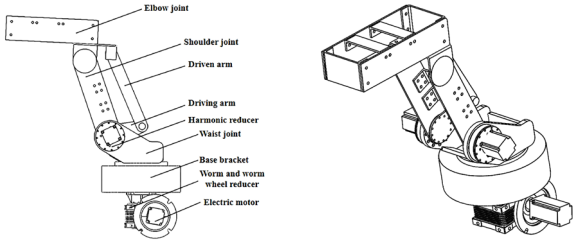

Fig. 7. Three-dimensional model of tomato picking robotic arm

4. Motion simulation analysis of tomato picking robotic arm

In this paper, the established three-dimensional model of the tomato picking robotic arm is imported into the Simulink simulation platform through the Simscape Multibody Link plugin. After adding the motion trajectory function, inverse solution function, clock module, signal input module, and data acquisition module, a motion simulation analysis is carried out on it. The block diagram of the motion simulation model is shown in Fig. 8.

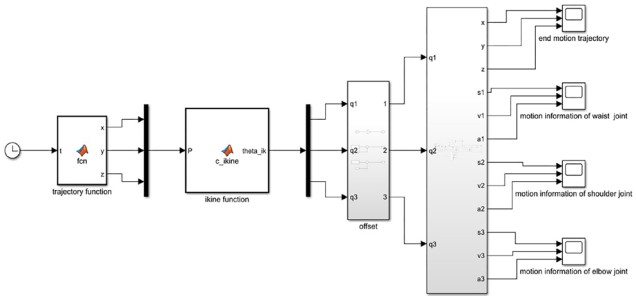

Fig. 8. Block diagram of the motion simulation model of the tomato picking robotic arm

After completing the construction of the motion simulation model for the tomato picking robotic arm, the simulation is started, and the robotic arm then operates according to the preset motion trajectory. The motion trajectory of the center point at the end of the tomato picking robotic arm and the motion characteristics of each rotating joint are shown in Fig. 9.

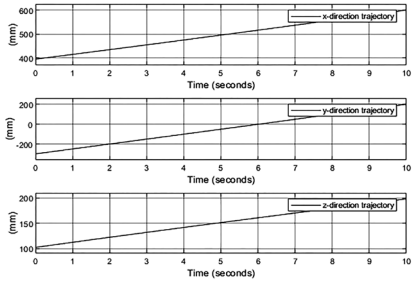

(a). End motion trajectory

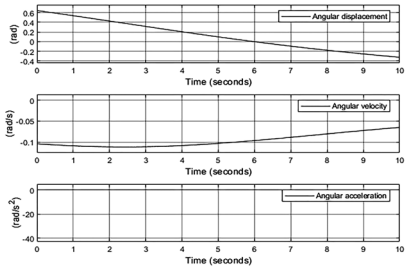

(b). Motion information of waist joint

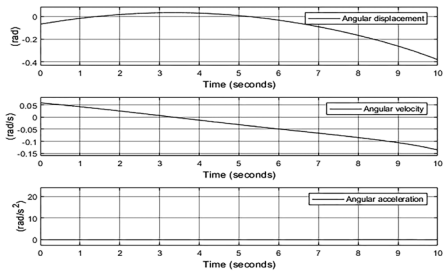

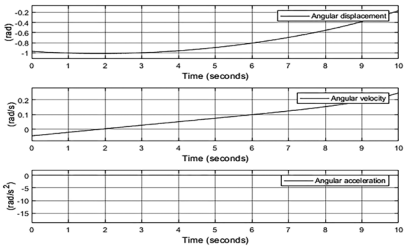

(c). Motion information of shoulder joint (b). Motion information of elbow joint

Fig. 9. Characteristic diagram of the motion simulation of the tomato picking robotic arm

According to the motion simulation characteristic diagram, it can be observed that the tomato picking robotic arm operates smoothly throughout the entire motion process, and there is no interference or collision among the various joints. The motion trajectory variation curves of the end of the tomato picking robotic arm in the x, y, and z directions are continuous and stable. The angular displacement, angular velocity, and angular acceleration variation curves of the three rotating joints of the tomato picking robotic arm are all continuous and smooth, without any abnormal sudden changes. This indicates that the overall motion of the tomato picking robotic arm is coherent and stable, with relatively high stability and controllability.

To verify whether the actual workspace of the tomato picking robotic arm meets the operational requirements and to evaluate its motion performance in practical applications, experiments on the workspace and motion performance were conducted using a physical prototype of the tomato picking robotic arm.

(1) Workspace experiment: Taking the position of the tomato picking robotic arm base as the origin and the center point of the end-effector as the target point, ten sets of target point positions were selected, covering extreme positions, intermediate transition positions, and random positions. By controlling the simulation system, the motors were driven to rotate specific angles to move the target points to the predetermined positions. The actual coordinates of the target points were measured and recorded. Part of the experimental process is shown in Fig. 10, and the experimental data is presented in Table 1.

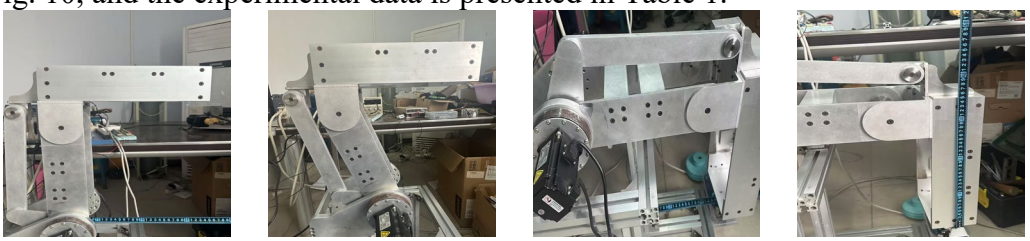

(a). Part of the experimental process 1 (b). Part of the experimental process 2 (c). Part of the experimental process 3 (d). Part of the experimental process 4

Fig. 10. Workspace testing process of the tomato picking robotic arm

Table 1

Workspace testing data of the tomato picking robotic arm

Group number	Target position(mm)	Actual position(mm)	Error(mm)
1	(700, 0, 100)	(696, 3, 104)	(4, -3, -4)
2	(-700, 0, 100)	(-703, 5, 105)	(3, -5, -5)
3	(0, 700, 100)	(-4,694,104)	(4, 6, -4)
4	(0, -700, 100)	(5, -696, 106)	(-5, -4, -6)
5	(0, 0, 800)	(6, 5, 795)	(-6, -5, 5)
6	(350, 0, -250)	(345,5, -246)	(5, -5, -4)
7	(350, 0, 450)	(415, 428, 352)	(-7, -6, -5)
8	(422, -422, 347)	(-5, 592, 354)	(5, 5, -7)
9	(-462, -462, 275)	(-456, -470, 280)	(-6, 8, -5)
10	(265, -265, 509)	(272, -260, 515)	(-7, -5, -6)

According to Table 1, the actual workspace range of the tomato picking robotic arm is essentially consistent with the simulated workspace range, and the errors between the target positions and the actual positions are all within 10 mm. This verifies that the workspace range and positioning accuracy of the tomato picking manipulator in practical applications meet the operational requirements.

(2) Motion performance test: Firstly, a motion trajectory is preset so that the simulation model and the physical prototype of the tomato picking robotic arm move from point A to point B in space, in order to obtain the simulated motion trajectory and the actual motion trajectory of the end of the tomato picking robotic arm. Subsequently, the simulated and actual motion trajectories are respectively compared with the theoretical motion trajectory. The motion performance of the tomato picking robotic arm is analyzed based on the comparison results. The comparison diagrams of the starting and ending position points between the model and the physical prototype are shown in Fig. 11, and the comparison of the end motion trajectories is shown in Fig. 12.

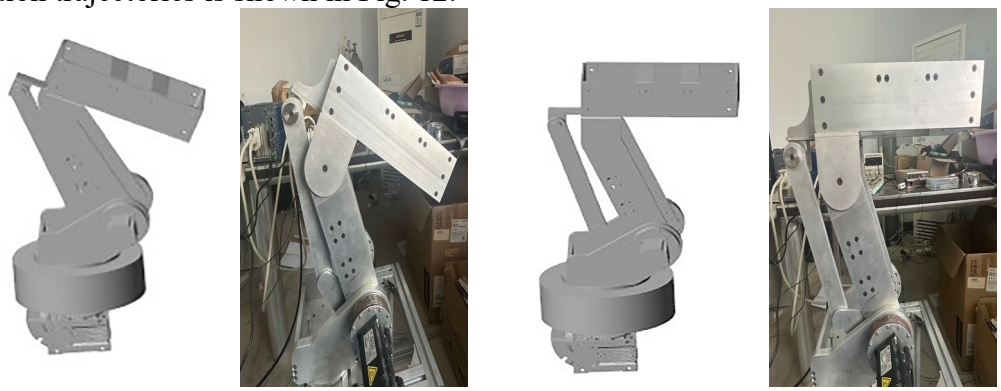

(a). Initial position (b). Terminal position

Fig. 11. Comparison diagram between the model and the actual object of the starting and ending position points

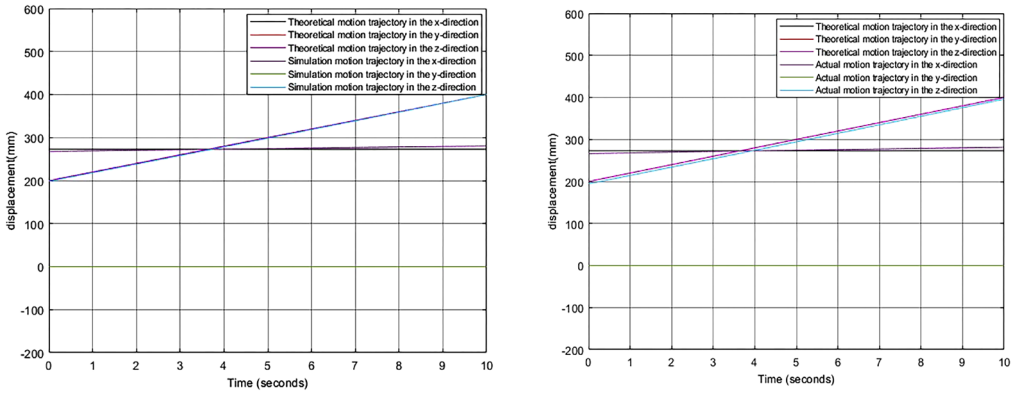

(a). Theory and simulation (b). Theory and actuality

Fig. 12. Comparison of the end motion trajectories

According to Fig. 12, the theoretical, simulated and actual motion trajectories at the end of the tomato picking robotic arm are roughly the same, continuous and stable, without any sudden changes. In the x direction, the simulated and actual motion trajectories have an error of approximately 3-5 mm compared to the theoretical motion trajectory. In the z direction, the actual motion trajectory has an error of approximately 2 mm compared to the theoretical motion trajectory. The reasons may be that errors occurred during the assembly of the robotic arm or rounding errors occurred during numerical calculations. Based on the above information and Fig. 11, it can be known that the tomato picking robotic arm can move smoothly according to the preset trajectory in actual work and has good motion performance.

5. Conclusions

Based on the self-developed visualization platform for personalized design of picking robotic arms, this paper optimizes and designs a tomato picking robotic arm suitable for greenhouse environments. The working range of the x-axis of the robotic arm is approximately [-700, 700] mm, the y-axis is approximately [-700, 700] mm, and the z-axis is approximately [-200, 800] mm, meeting the design requirements. Through kinematic simulation analysis and prototype testing of the tomato picking robotic arm, it is concluded that the motion trajectory change curves of the robotic arm's end in the x, y, and z directions are continuous and stable. The angular displacement, angular velocity, and angular acceleration change curves of the three rotational joints are all continuous and smooth without abnormal mutations. The actual working space range of the robotic arm is basically consistent with the simulated working space range. The error between the target position and the actual position is controlled within 10 mm, and the error between the simulated and actual motion trajectories and the theoretical motion trajectory is controlled within 5 mm. This proves that the tomato picking

robotic arm can move smoothly along the preset trajectory in actual work, and both the working space range and positioning accuracy meet the operational requirements.

REFERENCES

[1]. *C.J. Zhao, B.B. Fan, J. Li Q.C. Feng.* "Advances, Challenges and Trends of Agricultural Robot Technology, in Smart Agriculture (Chinese-English Version), Vol. **5**, Iss.4, 2023.

[2]. *J. Wang, T. Z. Guo, W. Chen, G. Yang Y. F. Zheng*, Kinematics Analysis and Simulation of Serial Robots for Fruit and Vegetable Picking, in Manufacturing Automation, Vol. **45**, Iss. 5, 2023.

[3]. *R. Oberti, A. Shapiro,* Advances in robotic agriculture for crops, in Biosystems Engineering, Vol. **146**, 2016.

[4]. *A. S. Konovalov, I. M. Kublin*, Agribusiness Robotization: Relevance, Development Prospects and Problems, in Questions of modern science and practice, Vol. **2**, Iss. 76, 2020.

[5]. *D. E. Fedorov*, Modern trends in developing robotic systems in agro-industrial complex, in IOP Conference Series: Earth and Environmental Science, Vol. **949**, Iss. 1, 2022.

[6]. *J. Davidson, C. J. Hohimer, C. Mo M. Karkee,* Dual Robot Coordination for Apple Harvesting, 2017 ASABE annual international meeting, American Society of Agricultural and Biological Engineers, 2017.

[7]. *A. Silwal, J. R. Davidson, M. Karkee, C. Mo, Q. Zhang K. Lewis*, Design, integration, and field evaluation of a robotic apple harvester", in Journal of Field Robotics, Vol. **34**, Iss. 2, 2017.

[8]. *K. Lammers, K. Zhang, K. Zhu, P. Chu, Z. Li R. Lu,* Development and evaluation of a dual-arm robotic apple harvesting system, in Computers And Electronics In Agriculture, Vol. **227**, part. 2, 2024.

[9]. *C. Lehnert, A. English, C. McCool, A. W. Tom T. Perez*. Autonomous Sweet Pepper Harvesting for Protected Cropping Systems, in IEEE Robotics and Automation Letters, Vol. **2**, Iss. 2, 2017.

[10]. *H. A. M. Williams, M. H. Jones, M. Nejati, M. J. Seabright, J. Bell, N. D. Penhall, J. J. Barnett, M. D. Duke, A. J. Scarfe, H. S. Ahn, J. Y. Lim, B. A. MacDonald*, Robotic kiwifruit harvesting using machine vision convolutional neural networks, and robotic arms, in Biosystems Engineering, Vol. **181**, 2019.

[11]. *S. Hayashi, S. Yamamoto, S. Tsubota, Y. Ochiai, K. Kobayashi, J. Kamata, M. Kurita, H. Inazumi R. Peter,* Automation technologies for strawberry harvesting and packing operations in Japan, in Journal of Berry Research, Vol. **4**, Iss. 1, 2014.

[12]. *M. H. Wang, Z. D. Zhou, Y. L. Wang, J. Xu, Y. J. Cui*, Design and experiment of facility elevated planting strawberry continuous picking manipulator, in Computers and Electronics in Agriculture, Vol. **228**, 2025.

[13]. *S. S. Mehta, T. F. Burks*, Vision-based control of robotic manipulator for citrus harvesting, in Computers and Electronics in Agriculture, Vol. **102**, 2014.

[14]. *E. J. V. Henten, D. A. V. Slot, C. W. J. Hot L. G. V. Willigenburg*, Optimal manipulator design for a cucumber harvesting robot, in Computers and Electronics in Agriculture, Vol. **65**, Iss. 2, 2009.

[15]. *F. Zhang, S. H. Zhang, J. X. Zhang, T. Yuan W. Li,* System Design of Greenhouse Cucumber Picking Robot, in Agricultural Engineering Technology, Vol. **40**, Iss. 25, 2020.

[16]. *Y. L. Yang, C. Y. Li*, Design and Experiment of Flexible Grape Picking Manipulator Based on SCARA, in Journal of Agricultural Mechanization Research, Vol. **47**, Iss. 01, 2025.

[17]. *Q. C. Wan, Z. M. Lu, X. X. Gao, C. H. Lu, X. Luo, J. Liao, A. Wan, X. B. Pang J. B. Xie*, Review on the Current Situation and Development of Fruit and Vegetable Picking Robots, in Digital Agriculture & Intelligent Agricultural Machinery, Iss. 3, 2024.